DIGITAL PHOTOGRAMMETRIC CAMERAS: A NEW FORWARD LOOKING APPROACH

Peter Fricker, Rainer Sandau, Peter Schreiber *

Abstract

Airborne digital sensors are already a reality. The transition from analytical to digital photogrammetry is well advanced and the dividing lines between photogrammetry and remote sensing grow increasingly blurred. One of the advantages of direct digital data capture in the air is the possibility of capturing multispectral data as well as panchromatic. Between modern film-based aerial mapping cameras with their extremely high resolution and, at the other end of the spectrum, the high-resolution satellite sensors, the market for new airborne devices is large and incontestable.

Two competing technologies are available as the basis for airborne digital sensors - linear and matrix array CCDs. The price/performance ratio of the matrix array CCDs are insufficient to offer swath widths and resolutions comparable to film cameras. The most promising alternative are linear arrays, arranged in a triplet on the focal plane, one forward-, one nadir- and one backward-looking. When combined with GPS and INS systems, this configuration provides geometric performance that enables the same photogrammetric operations to be performed on the workstation as with scanned film imagery. Additionally, multispectral CCD lines can be placed on the focal plane, providing data unique for remote sensing due to the additional advantages of geometrically correct sensor modeling, stereo imagery and accurate geo-coding.

A development project between LH Systems and the German Aerospace Centre has resulted in a functioning three-line sensor. An engineering model is being flown successfully and a production model was introduced to market in summer 2000 at the ISPRS congress in Amsterdam.

KEY WORDS: digital sensor, digital camera, inertial measurement, digital photogrammetry, multispectral imagery

1. INTRODUCTION

LH Systems' announcement at the end of 1998 that an engineering model of their forthcoming airborne digital sensor had been flown successfully implies that a genuine alternative to the familiar aerial film camera is imminent.

Except for producing stereoscopes, LH Systems and its predecessor Leica were never active in image interpretation. Yet this new sensor will have multispectral lines on the focal plane: it will be capable of generating precise,

* LH Systems GmbH, Switzerland

geometric information about the surface of the earth, but will also produce data amenable to proven remote sensing techniques. It will further soften the demarcation between photogrammetry and remote sensing and accelerate the decline of the photo laboratory, as digital image data can be transferred from the aircraft directly to the workstation.

The debate about airborne versus spaceborne imagery continues. The highest resolution applications, with ground pixel sizes in the one centimetre to one decimetre level, are likely to remain the province of the film camera. Yet there is a huge, pent up demand for top quality, multispectral information in the gap between this and the one metre and coarser resolutions offered by the satellite operators. Both spaceborne and airborne sensors have their advantages and the most likely scenario for the future will be an increased emphasis on data fusion as users select the sensors most likely to provide their information in each case and rely on their workstation software to use all the data together. The two types of data will be complementary rather than competitive.

2. AIRBORNE DIGITAL SENSORS: REQUIREMENTS

To have any chance of an impact in a market place spoilt for decades by high performance film cameras, an airborne digital sensor must provide:

- large field of view and swath width
- high resolution and accuracy, both geometric and radiometric
- linear sensor characteristics
- multispectral imagery
- stereo.

The first requirement, however, seems to rule out area CCD arrays, because readily available models in mid 1999 are 4Kx4K pixels or less, whereas a linear array of 12,000 pixels is readily available, requiring only one third as many flight lines. Considerable research work has been done in Germany since the 1970s, which has demonstrated the suitability of three panchromatic lines on the focal plane, with additional multispectral lines near the nadir. This obviates the need for multiple area arrays to provide a wide field of view and a multispectral capability (Figure 1). The left-hand diagram suggest how the focal plane could be populated using the three line principle: three panchromatic lines give the geometry and stereo, whilst additional lines, their sensitivity controlled by filters, give the multispectral information. In the right hand diagram, multiple area array CCDs and lenses are required to provide both the same ground pixel size and multispectral range as the three-line approach.

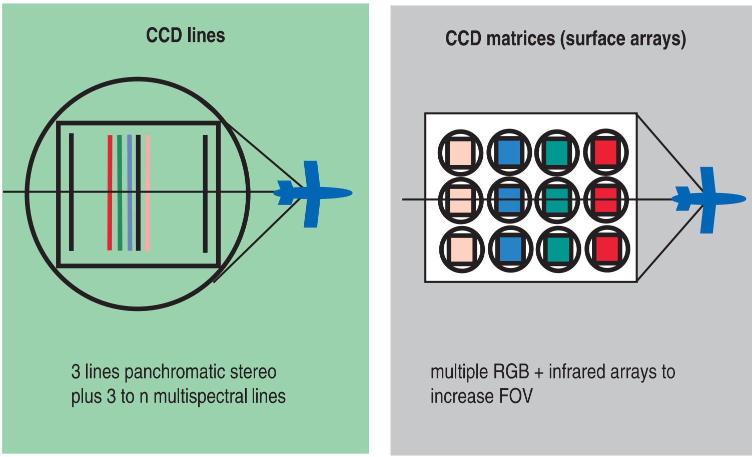

Figure 1: The alternatives: linear and area CCD arrays

3. THREE - LINE SCANNER APPROACH

The three-line concept results in views forward from the aircraft, vertically down and looking backward (Figure 2). The imagery from each scan line is assembled into strips (Figure 3). The characteristics of relief displacement in the line perspective geometry of the strip approach vis a vis the conventional central perspective geometry are indicated in Figure 4, showing the line perspective geometry of the three-line imagery on the left and the familiar central perspective geometry of the film photograph on the right. The angles between the incoming information to the three lines are, of course, fixed. With three lines there are three possible pairings for stereoscopic analysis - strips 1 and 2, 2 and 3, and 1 and 3. With film cameras, the parallactic angle is a function of principal distance and airbase. Moreover, every object appears on all three strips, whereas on film imagery only 60% of the area of any one photograph is in a triple overlap.

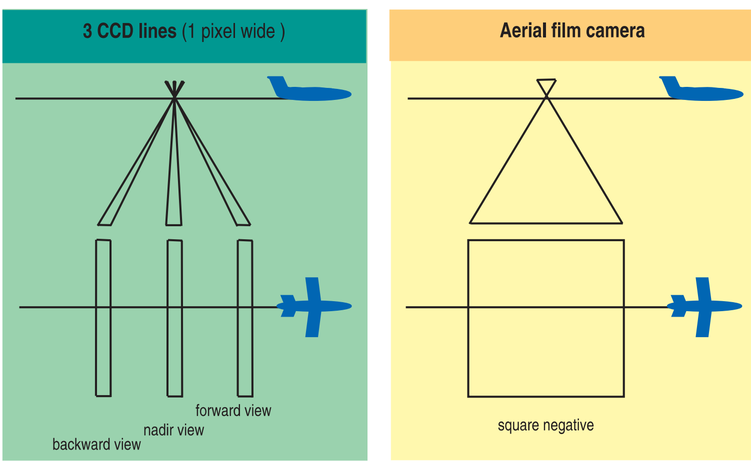

Figure 2: Basic geometric characteristics of three-line digital sensor and film camera

Figure 3: Comparison of the acquisition of scenes by three-line digital sensor and film camera

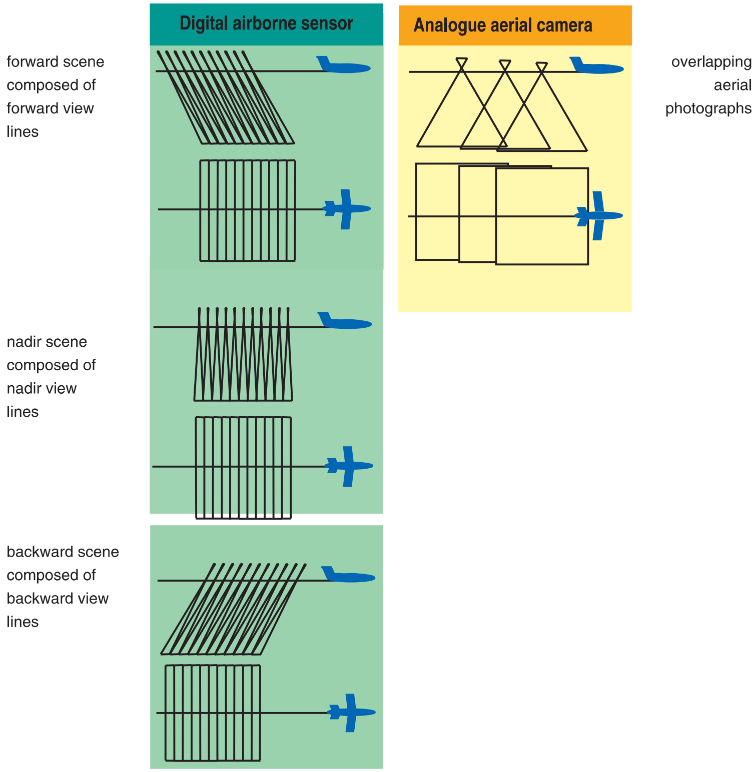

Figure 4: Effect of terrain relief on the imagery

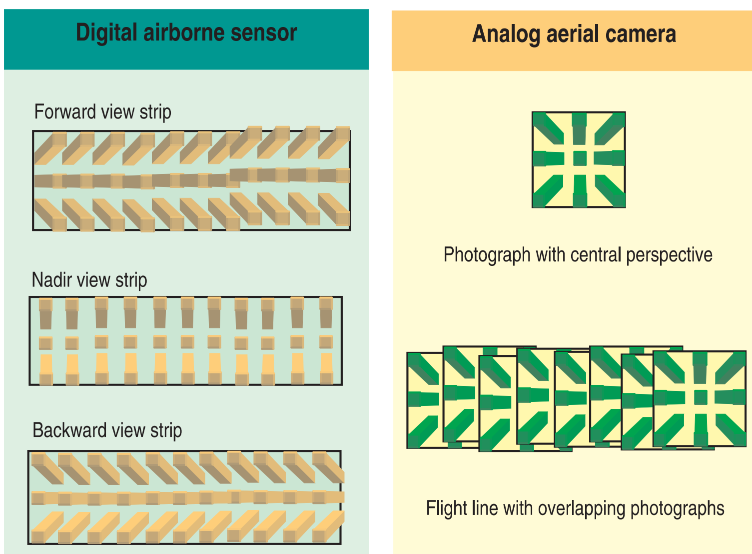

4. RADIOMETRIC CONSIDERATIONS

The best possible signal to noise ratio (SNR) is a precondition for signal processing, digitising, data compression and data transfer with little interference. The signal to noise ratio of the elements of a CCD are given by:

$$SNR = \frac{n_s}{\sqrt{\sigma_s^2 + \sigma_{rms}^2 + \sigma_{fp}^2}} \quad , \tag{1}$$

where n_s : signal electron count
σ_s^2 : variance of signal electron count
σ_{rms}^2 : variance of the time dependant noise
σ_{fp}^2 : variance of local sensitivity differences (fixed pattern noise).

The signal electron count is directly proportional to the number of arriving photons (within a defined narrow wavelength interval). The noise of the signal electrons therefore is subject to the Poisson statistics of photon noise:

$$\sigma_s = \sqrt{n_s} \quad . \tag{2}$$

The time dependent noise of the CCD and of the analogue channel (rms noise) contains:

- temporary dark signal noise (Poisson statistic)
- reset-noise and on-chip-amplifier noise ("kTC-noise")
- transfer noise
- other electronic noise (1/f - noise, thermal noise).

For estimation purposes the following calculations are based on a noise electron count of

$$\sigma_{rms} = 235e^- \quad .$$

The fixed pattern noise has two sources

- photo response non-uniformity (PRNU) of the CCD elements
- shading of the light intensity in the focal plane of a wide-angle optics.

Observing the behaviour of only one CCD element by ignoring the PRNU (photo response non-uniformity), e.g. the fixed pattern noise, we find the conditions shown in Figure 5, if we take into account a saturation electron count of >500.000. The SNR amounts to 8 or 9 bits (SNR = 250 ... 670) for an electron count >100.000.

If we now look at the real conditions in the focal plane of a wide-angle lens, we obtain the diagram of the signals at the outlet of a CCD line, as shown in Figure 6: flat field illumination creates in the focal plane of wide-angle optics a CCD signal including the effects of shading due to optics and PRNU.

Figure 5: SNR of a CCD-element at a saturation load of 500.000 electrons and rms-noise of 235 electrons

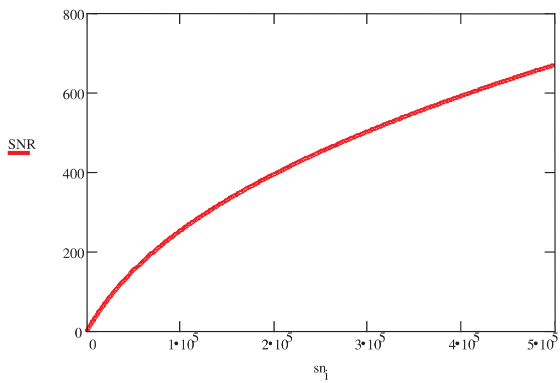

Figure 6: Effect of flat field illumination in the focal plane

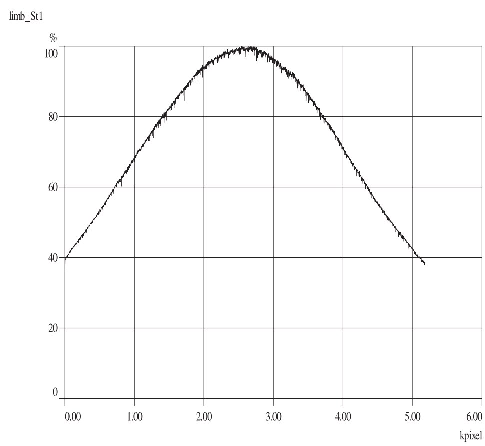

One can clearly see the effect of the shading of the lens (at the edges the light intensity falls off to about 40%) and of the influence of the PRNU. The differences of sensitivity of CCDs are usually indicated in the datasheets as PRNU values in percent of the values of the videocurrent for the range far below saturation (mostly at 50% of). We will adhere to this definition here as well. Thus in the linear range of the CCD the fixed pattern noise of the pixel sensitivity can be expressed directly as a signal dependent noise, which is converted into a time dependent noise during transfer of the charge.

$$\sigma_{fp} = \frac{PRNU}{100\%} \cdot n_s = \frac{PRNU}{100\%} \cdot \sigma_s^2 \quad . \tag{3}$$

Depending on the PRNU of the CCD the signal to noise ratio results as:

$$SNR = \frac{\sigma_s}{\sqrt{1 + \left[\frac{PRNU}{100\%} \cdot \sigma_s\right]^2 + \left[\frac{\sigma_{rms}}{\sigma_s}\right]^2}} \quad . \tag{4}$$

Figure 7 shows the highest attainable SNR at full exploitation close to saturation (400.000 to 500.000 signal electrons) in relation to PRNU, based on the aforementioned parameters. Up to a PRNU value of 0.02% the SNR is determined exclusively by the photon noise of the signal, the rms noise of the CCD and the noise of the analogue channel. At 0.1% the PRNU influence becomes dominant. In the engineering model of LH Systems' new airborne digital sensor, described in sections 6 and 7 below, the PRNU correction is done pixel-wise.

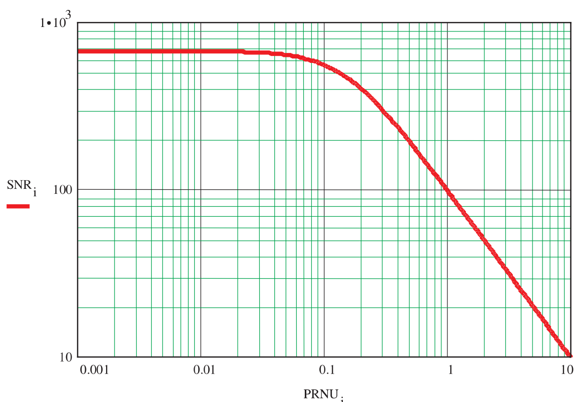

Figure 7: SNR in relation to PRNU assuming a thermal and electronic noise of Sel = 235 rms-electrons and a signal electron counts of 500.000 e-

Normally light fall-off of the lens system (approximately 30%) is corrected simultaneously with the PRNU correction. For the estimation or the PRNU correction, this fall-off has not been taken into account because it does not contribute directly to an increase of the SNR. It only contributes indirectly through the adaptation of the signal to the analogue channel. The correction of light fall-off of the lens does not restrict the SNR significantly.

The efficiency of the correction can be seen in Figure 8, which shows imagery of the Reichstag, Berlin, taken with the engineering model of the LH Systems airborne digital sensor on 23 April 1999. The flying height was 3 km and the ground sample distance is 0.25 m. In the radiometrically zoomed-out image parts no noise can be seen.

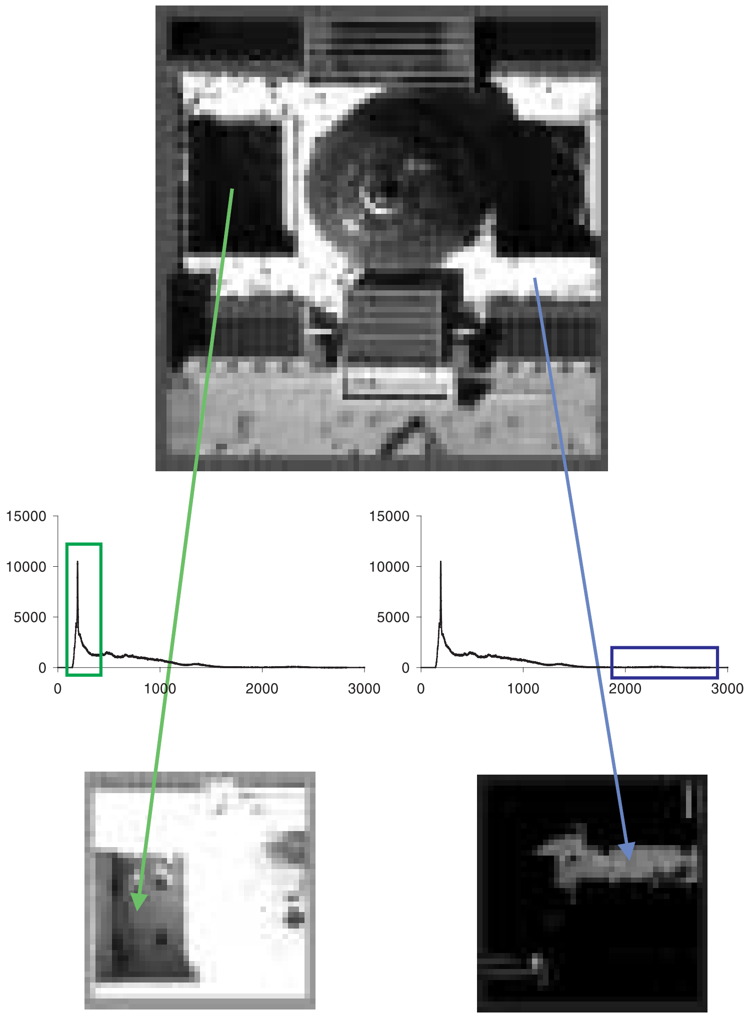

Figure 8: Imagery of Berlin, taken with the engineering model of the LH Systems airborne digital sensor.

5. MTF CONSIDERATIONS

The geometrical resolution of the camera system essentially depends on the MTF of the system optics/CCD pixel. It describes the damping of the incoming radiation as a function of the spatial frequency. This may serve as a basis to define a contrast function.

Considering only this optics/CCD-pixel system, the MTF_{SYS} is calculated by multiplying the MTFs of the system constituents MTF_{OPTICS} and MTF_{PIXEL}

$$MTF_{SYS} = MTF_{OPTICS} * MTF_{PIXEL} \quad . \tag{5}$$

The MTF_{PIXEL} of the CCD pixel is:

$$MTF_{PIXEL} = \frac{\sin(\pi \cdot k \cdot x)}{(\pi \cdot k \cdot x)} \quad , \tag{6}$$

with k being the spatial frequency measurement in mm-1 and Δ being the pixel distance, here 6.5 µm.

The function MTF_{PIXEL} is shown in Figure 9.

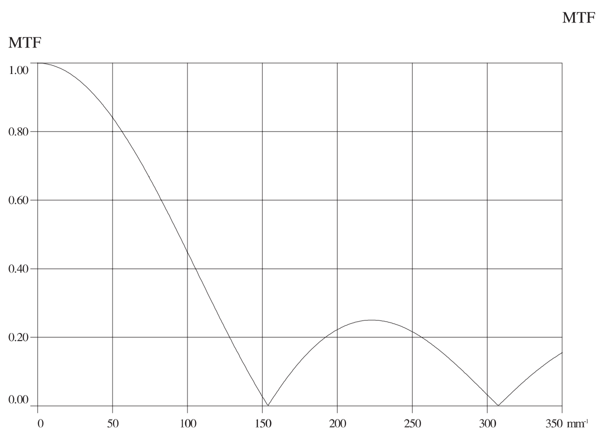

Figure 9: MTF of CCD pixel, distance of pixel centers 6.5 µm

Figure 10: MTF_{OPTICS} of MTF_{SYS} of the engineering model (EM) at the optical axis

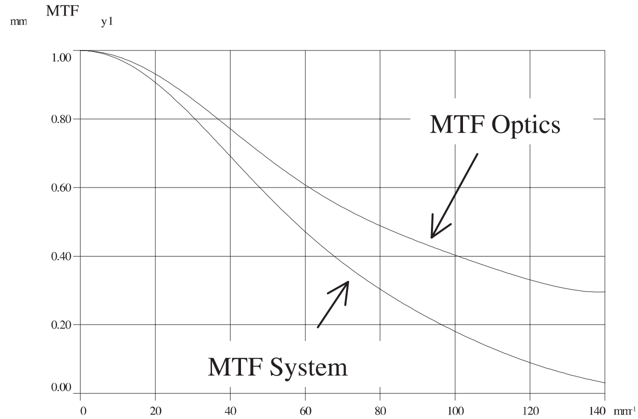

This Figure shows the MTF_{OPTICS} of the EM optics measured in the optical axis of the calibration

laboratory of the DLR Institute for Space Sensor Technology in Berlin, Adlershof. The second curve in Figure 10 is the resulting MTF_{SYS} for the nadir looking pixel.

To allow for comparison with the MTF of the pixel given in Figure 9, a wider range of MTF_{SYS} is shown in Figure 11.

Figure 11: MTF of a pixel near the optical axis of the engineering model

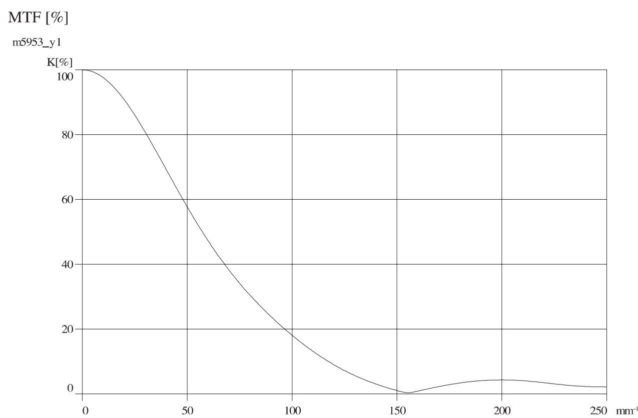

With a MTF_{SYS} of 30% at the Nyquist frequency:

$$k_{NY} = \frac{1}{2\Delta} \quad , \tag{7}$$

given for Δ = 6.5 mm, a number of k_{NY} = 77 Lp/mm (Line pairs per mm), the contrast potential and therefore the imaging quality of the EM is pretty good. This holds also for the non-nadir areas of the focal plane used by the nadir and stereo looking CCD lines, since the MTFSYS does not deviate dramatically form the shown curve. Figure 12 gives a measured curve for the centre of the stereo forward line (17° stereo angle) in comparison with the centre of the nadir line.

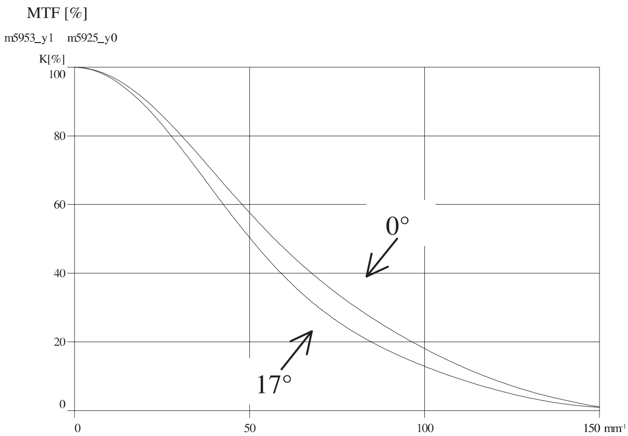

Figure 12: MTF of centre of nadir line (0°) and centre of forward stereo line (at 17° stereo angle)

6. IMAGE PROCESSING

The raw imagery looks bizarre, because aircraft tilts and terrain relief cause the linear arrays to image widely varying strips of terrain, which is well known. Fig. 13 shows imagery acquired by the nadir sensor of the new camera over Berlin. The flight direction was from left to right. The top image is raw. The bottom image has been rectified and looks similar to a conventional aerial photograph. Note the correspondence between the edges of the rectified image and the roll of the aircraft. Tilts have been compensated by adjusting each individual scan line for the attitude of the aircraft, using data from the airborne GPS and INS units carried on every fight. An initial rectification using these data is essential even to view the imagery. Thereafter, operations such as triangulation, DTM measurement, orthophotos and feature extraction continue in the usual way. Automated processes, such as point measurement for triangulation and DTM extraction, can be based on triplet matching using the three strips.

Owing to their positions on the focal plane, combined with the aircraft and terrain variations, the colour lines image slightly different parts of the earth's surface. Thus full rectification is required, i.e. orthophotos are produced, before the colour bands can be properly registered and transformed into colour composite images suitable for analysis by off-the-shelf remote sensing packages.

Figure 13: Imagery acquired by the new sensor over Berlin

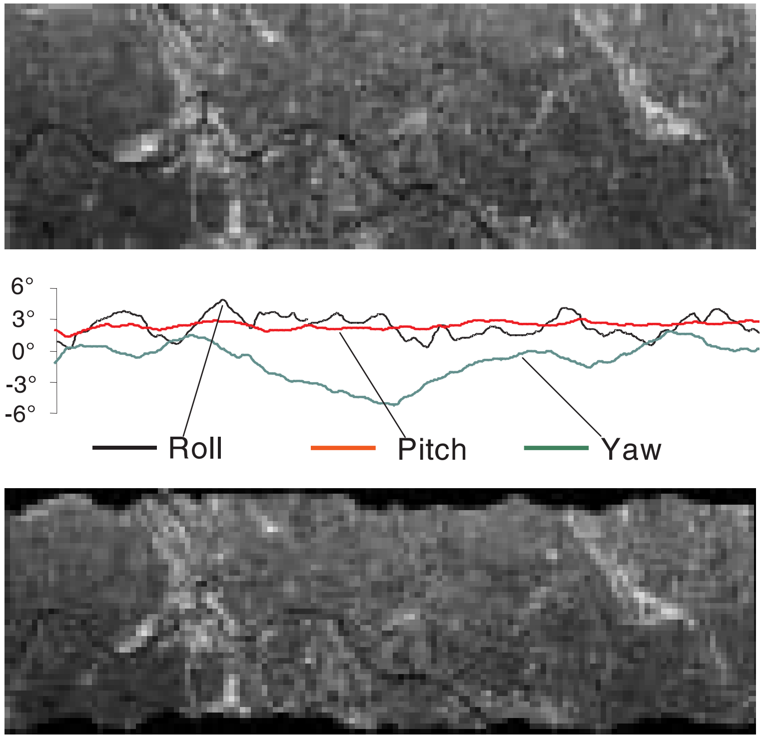

7. ENGINEERING MODEL (EM) AND TECHNICAL CO-OPERATION

The complexity, cost and difficulty of developing and manufacturing a novel airborne digital sensor ruled out "going it alone". In early 1997, shortly before LH Systems was formed, Leica Geosystems reached a technology agreement with Deutsches Zentrum für Luft und Raumfahrt (DLR), the German Aerospace Centre in Berlin. This provided for long term co-operation, with joint development by both parties and assembly by Leica Geosystems. DLR's experience in this area is unparalleled. Amongst a host of intricate and impressive achievements in both airborne and spaceborne technology, it made historic progress with sensors based on the three-line approach, for example the WAOSS (Wide Angle Optical Stereo Sensor, built for the unfortunate Mars-96 mission) (Sandau and Bärwald, 1994), WAAC (Wide Angle Airborne Camera) (Sandau and Eckhardt, 1996) and HRSC (High Resolution Stereo Camera) (Albertz et al., 1996). DLR's expertise complemented well Leica Geosystems' abilities in optics, mechanics and electronics, together with its deep appreciation of customers' requirements acquired through decades of producing aerial film cameras. It was natural that the agreement between the parties be transferred to LH Systems quite soon after its formation.

8. IMU AND GPS INTEGRATION

In order to reconstruct high-resolution images from line scanner data, the orientation data of each line has to be obtained. The inventors of the three-line principle proved mathematically that this could be done by using observations from image matching techniques only, as provided in modern aerotriangulation packages. But computation time required for this indirect method is so large, that direct observations from attitude and position sensors are seen as the easiest way to reduce processing time. Applying only the indirect method is time consuming; applying only the direct method is capital intensive. The decision was made to find an optimal trade-off by including direct measurements from GPS and IMU sensors of only certain accuracy into the aerotriangulation techniques. The advantages of this trade-off are:

- data processing time to rectify line scanner data is reduced significantly,
- price/performance ratio of medium priced IMU sensors is likely to improve faster over time.

The tight integration (Fig. 14) with the focal plane of a digital line sensor has a large potential for further reduction of ground control.

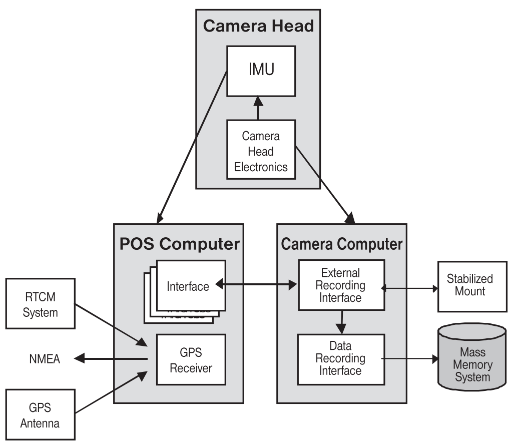

Figure 14: Main components of tight integration of IMU/GPS and a three-line sensor camera

In 1998 LH Systems and Applanix Corporation from Canada set up a working group to analyse the potential and propose solutions to achieve a tight integration between IMU, GPS and line sensors, within the scope of the co-operation agreement that LH Systems has with DLR. As one of the results, the engineering model of the airborne digital sensor is now being flown routinely including IMU and GPS sensors from Applanix Corporation.

9. PRACTICAL CONCLUSIONS

The features of the film and digital approaches are compared in Table 1. LH Systems has chosen the three-line scanner approach for the reasons given above. The engineering model (EM) has flown (see Fig. 15, Table 2) and work is proceeding towards the production model, which will have at least 20.000 pixels in each line, faster integration times and multispectral bands. It was launched at the ISPRS Congress in Amsterdam.

Photogrammetrists will be able to share data with the remote sensing community and for the first time create deliverables with both the depth of information accruing from image understanding of multispectral images and the geometric fidelity of photogrammetry. In the standard version of the new airborne digital sensor the multispectral images will be derived from the data captured with four CCD sensors equipped with appropriate filters in the RGB and NIR bands. These data will be used to produce true-colour and false-colour composites based on the orthophotos derived from the panchromatic three-line CCD sensors.

Table 1: Features of aerial film camera and airborne digital sensor

Characteristic	Aerial film camera	Airborne digital sensor
Flying time	80%	100%
Photo lab	Yes	Unnecessary
12-bit in-flight sensing	No	Yes
8/10-bit scanning	Yes	Unnecessary
Data volume	80-50%	100%
Pre-processing	No	Yes
GPS	Yes (optional)	Very useful
INS	Unusual	Very useful
Projection centres	Interpolated (few)	Interpolated (many)
Ground control points	Yes, but few when using GPS	Yes, but fewer with INS/ GPS
Tie point matching	Few – between images	Many

It is LH Systems' intention to make the image data format accessible to all third party remote sensing software packages used for image enhancement and image analysis. SOCET Set software will provide basic image enhancement functions.

General	
Principle	three-line CCD stereo sensor
Pixels per CCD Line	12,000
Pixel size	6.5 µm
Dynamic range	12 bit (raw data mode)
Radiometric resolution	8 bit
Normalisation mode	8 bit linear or non-linear
FOV (across track)	52°
Focal length	80 mm
Swath at 10,000' flying height (3,100 m)	3,000m (1.9 miles) and 25 cm ground pixel size
Stereo angles	17°, 25°, 42°
Recording interval per line	1.2 ms
Filter range (at λ50)	Panchromatic, 465nm – 680nm

Power	
Input voltage	28 VDC or 220 VAC/50 Hz
Power consumption: average /(peak)	Engineering model: 600 W /(1000 W)
	Mass memory: 600 W /(600 W)
	ASCOT: 80 W /(180 W)

Table 2: Specifications of the engineering model

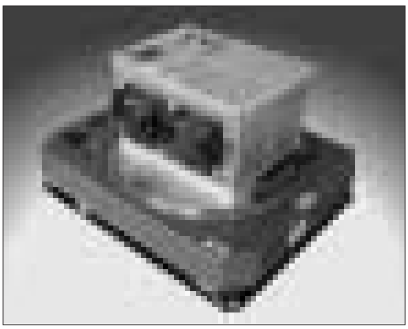

Figure 15: The engineering model of LH Systems' airborne digital sensor, which was successfully flown in late 1998.

ACKNOWLEDGMENTS

The authors thank DLR for its contributions to the development of the engineering model and the test flights. We owe special thanks to Dr. Reinhard Schuster who provided the engineering model calibration results used in this paper.

References

Albertz, J., Ebner, H. & Neukum, *G., 1996. The HRSC/WAOSS camera experiment on the MARS96 mission - A photogrammetric and cartographic view of the project. ISPRS Congress, Vienna, July 9-14.*

Sandau, R. and Bärwald, W., *1994. A three-line wide-angle CCD stereo camera for Mars-94 mission. In: International Archives of Photogrammetry and Remote Sensing, Vol. 30, Part B1, pp. 82-86.*

Sandau, R. and Eckardt, A., *1996. The stereo camera family WAOSS/WAAC for spaceborne/airborne applications. In: International Archives of Photogrammetry and Remote Sensing, Vol. 31, Part B1, pp. 170-175.*

Review: Editorial board ISPRS Ljubljana, February 2000

Received for the publication: 2000-05-11